

GaAs/AlGaAs quantum well and modulation-doped heterostructures grown by organometallic vapor phase epitaxy using trimethylamine alane

W. S. Hobson, F. Ren, M. Lamont Schnoes, S. K. Sputz, T. D. Harris, S. J. Pearton, and C. R. Abernathy
AT&T Bell Laboratories, 600 Mountain Avenue, Murray Hill, New Jersey 07974

K. S. Jones
University of Florida, Department of Materials Science, 214A Rhines Hall, Gainesville, Florida 32611

(Received 10 June 1991; accepted for publication 29 July 1991)

High-quality GaAs/AlGaAs quantum well and modulation-doped heterostructures have been grown by low-pressure organometallic vapor phase epitaxy (OMVPE) using trimethylamine alane (TMAA) as a new aluminum source. TMAA is an alternative to the conventional organometallic precursors and offers the advantage of substantially reduced oxygen and carbon incorporation in AlGaAs. Intense photoluminescence (PL) with narrow linewidths at 2 K was observed from multiple quantum well samples with well widths of 1.5–10 nm. Transmission electron microscopy of a fifty period superlattice (4 nm GaAs/44 nm $\text{Al}_{0.18}\text{Ga}_{0.82}\text{As}$) revealed abrupt interfaces and excellent well-to-well thickness uniformity. Selectively doped heterostructure transistors (SDHTs) fabricated on the modulation-doped structures exhibited a maximum extrinsic transconductance of 339 mS/mm for a 1- μm -gate length at 300-K, the highest reported for OMVPE grown devices. A unity current gain cutoff frequency, f_c , of 16 GHz and a maximum frequency of oscillation, f_{max} , of 23 GHz were obtained for these SDHTs.

Trimethylamine alane (TMAA), $(\text{CH}_3)_3\text{N}\cdot\text{AlH}_3$, is a potentially useful aluminum source for III–V epitaxy, as first demonstrated by Abernathy *et al.*¹ They utilized TMAA in conjunction with triethylgallium (TEGa) to grow high quality AlGaAs by metalorganic molecular beam epitaxy (MOMBE). The carbon and oxygen concentrations were significantly reduced in comparison to AlGaAs grown using the conventional organometallic Al sources. This is believed to result from the lack of a direct aluminum–carbon bond in TMAA, and from the inability of TMAA to form volatile aluminum alkoxides which are a source of oxygen. TMAA was subsequently explored as a possible aluminum source for organometallic vapor phase epitaxy (OMVPE).^{2–8} Extremely low carbon^{3–6} and oxygen⁷ concentrations were demonstrated in the growth of AlGaAs. To date, device demonstrations have included high-performance heterojunction bipolar transistors grown by MOMBE⁹ and low threshold GaAs/AlGaAs single quantum well graded-index separate confinement heterostructure lasers by OMVPE.^{5,7}

We report here on the utility of TMAA in conjunction with TEGa for the growth of GaAs/AlGaAs quantum well (QW) and modulation-doped heterostructures as examples of the types of layers used for optical and electronic devices. A GaAs/AlGaAs QW sample grown using the combination of TMAA and trimethylgallium was previously examined by photoluminescence (PL).² The combination of TMAA and TEGa, as employed here, should lead to superior QWs due to the significantly lower carbon present in the AlGaAs barriers.^{3,5} The structures have been characterized by PL, photoluminescence excitation (PLE), and transmission electron microscopy (TEM). Selectively doped heterostructure transistors (SDHTs) have also been fabricated. We find that the QWs exhibit intense

low-temperature (2 K) PL, narrow PL linewidths, and excellent well-to-well thickness uniformity. Maximum extrinsic transconductance of the SDHTs was 339 mS mm^{-1} for the 1- μm -gate length at 300 K.

Growth of the epitaxial layers took place in a low-pressure (30 Torr) OMVPE reactor described previously.⁶ The carrier gas was hydrogen and the source reagents were arsine, TEGa, and TMAA. Disilane was utilized for silicon doping. The reactor design was critical due to the low decomposition temperature (ca. 100 °C) of TMAA. Under our conditions, the gas velocity was sufficiently high so that no predeposition was observed upstream of the wafer. The TMAA was supplied as bis- $[(\text{CH}_3)_3\text{N}]_2\cdot\text{AlH}_3$ in a conventional stainless-steel bubbler.¹⁰

Some of the properties of thick epitaxial $\text{Al}_x\text{Ga}_{1-x}\text{As}$ layers grown using TMAA have been described previously,^{5–8} and are summarized briefly here for the readers' benefit. Over the entire compositional range ($x = 0.1$ – 1.0), the surfaces exhibited featureless morphology when examined by Nomarski differential interference contrast microscopy. The compositional uniformity of the $\text{Al}_x\text{Ga}_{1-x}\text{As}$ was exceptionally good for the lower Al mole fractions used here, e.g., $x = 0.24 \pm 0.002$ across a 40-mm diam.⁶ At higher Al mole fractions the nonuniformity increased, e.g., $x = 0.50 \pm 0.02$ over a similar area. Intense PL was observed at room temperature for AlGaAs compositions with direct band gaps ($x < 0.4$). Low-temperature (2 K) PL verified that the background carbon was present at very low concentration ($< 10^{16} \text{ cm}^{-3}$) based on the large relative intensity of the bound exciton compared to the nonexciton emission. The background doping level as determined from Hall measurements was typically below 10^{14} cm^{-3} for unintentionally doped AlGaAs. Deep-level transient spectroscopy on intentionally Si-doped

$\text{Al}_x\text{Ga}_{1-x}\text{As}$ ($N_D - N_A \sim 1-9 \times 10^{16} \text{ cm}^{-3}$, $0.2 < x < 0.5$) indicated the expected DX center and low concentrations of EL2 ($< 10^{13} \text{ cm}^{-3}$).¹¹ All other trap concentrations were below the detection limit ($\sim 10^{11}-10^{12} \text{ cm}^{-3}$), suggesting that TMAA does not introduce traps associated with oxygen. Secondary ion mass spectrometry measurements of $\text{Al}_{0.45}\text{Ga}_{0.55}\text{As}$ layers verified that the oxygen concentration was below the detection limit of $5 \times 10^{16} \text{ cm}^{-3}$, which is the lowest level achieved in AlGaAs grown by any technique.⁷

A multiple QW sample was grown at 650°C without the use of growth interruptions. The GaAs growth rate was 21 nm min^{-1} and the $\text{Al}_{0.32}\text{Ga}_{0.68}\text{As}$ barriers were 43 nm thick. An AsH_3 mole fraction of 7.5×10^{-3} was used. Shown in Fig. 1 is the corrected spectrum for the multiple QW structure; the calculated QW thickness (L_z) and the full width at half maximum (FWHM) for each well is also indicated. The calculation assumes a perfect square well, an exciton binding energy of 8 meV and a 60/40 band offset, and includes band nonparabolicity. Intense PL with narrow linewidths was observed, indicative of a long exciton lifetime in the QWs. The usual increase in the PL linewidth with decreasing L_z was also obtained. The FWHM of the widest well ($\sim 10 \text{ nm}$) is only 2.5 meV and compares favorably with values typically obtained from QWs grown by OMVPE. For example, Moshevskii *et al.*¹² reported a FWHM of 6.4 meV for a 10 nm QW with $\text{Al}_{0.3}\text{Ga}_{0.7}\text{As}$ barriers, and Schmitz *et al.*¹³ obtained a value of 6.7 meV nominally for the same structure. Schmitz *et al.*¹³ also reported a FWHM of 10.3 meV for a 2.5 nm QW and 12.2 meV for a 1.0 nm QW which again are somewhat broader than the values reported here for our 2.7 and 1.4 nm QWs.

A further indication of high quality QWs was the PLE spectra. The spectra for the 6.9 and 4.7 nm QWs, along with the corresponding PL, are shown in Figs. 2(a) and 2(b), respectively. The Stokes shifts are small, 2 and 6 meV , and the relative intensity of the heavy and light hole

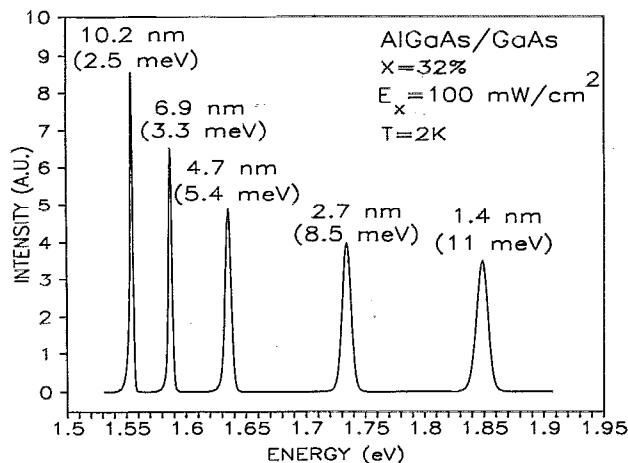


FIG. 1. Low-temperature (2 K) PL spectrum of a multiple QW sample with 43 nm $\text{Al}_{0.32}\text{Ga}_{0.68}\text{As}$ barriers. The calculated QW thicknesses and full width at half maxima are indicated adjacent to the associated QW PL peaks.

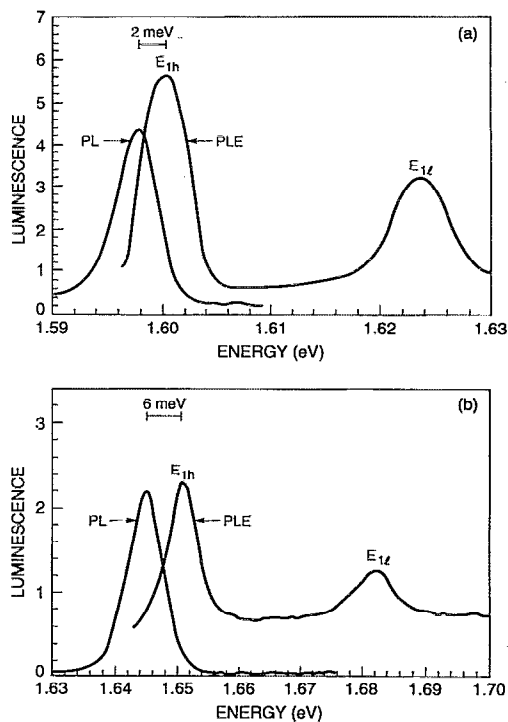


FIG. 2. Low-temperature (6 K) PL and PLE spectra of 6.9 nm (a) and 4.7 nm (b) QWs.

transitions is close to the expected 3-1 ratio. These two observations taken together suggest that there are extremely low concentrations of residual carriers in the wells. Also indicative of the absence of residual carriers is the nearly flat baseline under both PLE spectra. OMVPE growth of AlGaAs heterostructure barriers using alkyl-aluminum sources invariably results in substantial p -type residual doping. The use of TMAA results in lower residual impurities and allows the growth of QWs superior to those grown by OMVPE using conventional sources and approaching the best grown by MBE.

Presented in Fig. 3 is a TEM micrograph of a section from a fifty period superlattice consisting of 4.0 nm GaAs and 44 nm $\text{Al}_{0.18}\text{Ga}_{0.82}\text{As}$ layers grown at 700°C . The TEM micrograph was taken on a JEOL 4000 FX TEM using g_{200} centered dark field imaging conditions. To be noted are the abrupt interfaces, the absence of structural defects, and the excellent well-to-well thickness uniformity. This held true for the entire structure, and indicates that reproducible layers with abrupt interfaces can be produced using TMAA.

The layer structure of the SDHT, grown at 650°C , consists of a ten period (8 nm) AlGaAs/GaAs superlattice buffer, followed by a 300-nm GaAs channel layer, 2.5-nm $\text{Al}_{0.25}\text{Ga}_{0.75}\text{As}$ spacer, 35 nm Si-doped ($n = 2 \times 10^{18} \text{ cm}^{-3}$) $\text{Al}_{0.25}\text{Ga}_{0.75}\text{As}$ donor layer, and a 50 nm Si-doped ($n = 5 \times 10^{18} \text{ cm}^{-3}$) GaAs capping layer. Samples without this n^+ GaAs cap and with AlGaAs spacer thicknesses of 15 nm showed 77 K Hall mobilities of $76\,000 \text{ cm}^2/\text{V s}$ with a sheet carrier density of $8.9 \times 10^{11} \text{ cm}^{-2}$. The processing details for SDHTs have been described previously.¹⁴ Shown in Fig. 4 is the extrinsic transconduc-

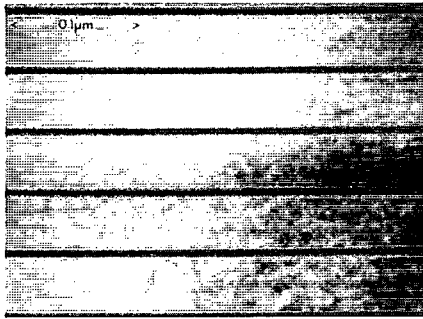


FIG. 3. A TEM micrograph taken using g_{200} centered dark field imaging conditions of a section from a fifty period superlattice consisting of 4.0 nm GaAs and 44 nm $\text{Al}_{0.18}\text{Ga}_{0.82}\text{As}$ layers.

tance, g_m , and drain current, I_D , as a function of gate bias, V_g , for a device with a 1.0- μm gate length. A maximum g_m of 339 mS mm^{-1} was obtained at $V_g = 0.58 \text{ V}$ with $I_D = 8.5 \text{ mA}$. This compares favorably with the previously best g_m of 330 mS mm^{-1} for 1.0- μm -gate length SDHTs grown by OMVPE using TEGa and triethylaluminum to suppress carbon incorporation in the AlGaAs layers.¹⁵ The device exhibits excellent pinch-off characteristics as shown in Fig. 4. The microwave characteristics of the SDHT were measured using Cascade microtech probes. Figure 5 shows the frequency dependence of the current gain, h_{21} , maximum stable power gain (MSG), and maximum available power gain (MAG) at room temperature for $V_G = 0.58 \text{ V}$. The unity current gain cutoff frequency, f_T , and power-gain cutoff frequency, f_{max} , were 16 and 23 GHz, respectively. The value of f_T is slightly lower than the best reported previously for the 1.0- μm gate length ($\sim 18 \text{ GHz}$),¹⁶ and is attributed to the high doping in the AlGaAs donor layer and the associated increase in gate-source capacitance.

In summary, we have demonstrated the utility of TMAA for the growth of high-quality QWs and modulation doped GaAs/AlGaAs heterostructures. High-performance SDHTs with a g_m of 339 mS mm^{-1} have been fab-

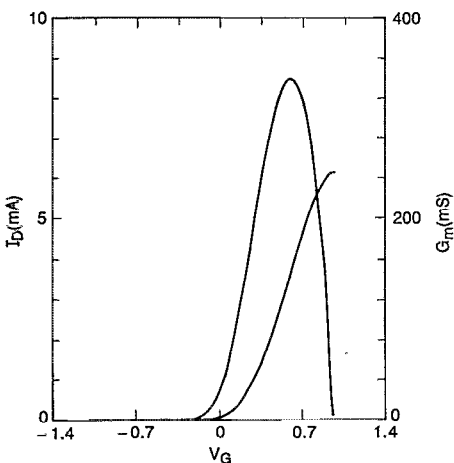


FIG. 4. Extrinsic transconductance, g_m , as a function of gate bias, V_g , for the SDHT at room temperature. The gate length was 1.0 μm . A maximum g_m of 339 mS mm^{-1} was obtained at $V_g = 0.58 \text{ V}$.

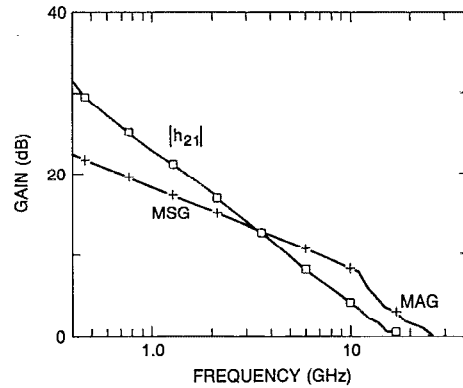


FIG. 5. Frequency dependence of current gain h_{21} , maximum stable power gain (MSG), and maximum available power gain (MAG) for the 1.0- μm -gate length SDHT at room temperature.

ricated. TMAA offers substantial advantages over trimethylaluminum for low-pressure OMVPE due to the reduced carbon and oxygen incorporation in AlGaAs. A major consideration is the avoidance of prereaction and/or predeposition of TMAA upstream of the wafer. We have accomplished this through the use of a single wafer vertical reactor operated at 30 Torr.

We wish to acknowledge L. J. Oster for technical assistance, Dr. Y. K. Chen for microwave measurements, and Dr. W. P. Weiner of American Cyanamid Company for useful discussions concerning trimethylamine alane.

- ¹C. R. Abernathy, A. S. Jordan, S. J. Pearton, W. S. Hobson, D. A. Bohling, and G. T. Muhr, *Appl. Phys. Lett.* **56**, 2654 (1990).
- ²J. S. Roberts, C. C. Button, J. P. R. David, A. C. Jones, and S. A. Rushworth, *J. Cryst. Growth* **104**, 857 (1990).
- ³A. C. Jones and S. A. Rushworth, *J. Cryst. Growth* **106**, 253 (1990).
- ⁴A. C. Jones and S. A. Rushworth, *J. Cryst. Growth* **107**, 350 (1991).
- ⁵W. S. Hobson, A. F. J. Levi, J. O'Gorman, S. J. Pearton, C. R. Abernathy, and V. Swaminathan, *Electron. Lett.* **26**, 1762 (1990).
- ⁶W. S. Hobson, T. D. Harris, C. R. Abernathy, and S. J. Pearton, *Appl. Phys. Lett.* **58**, 77 (1991).
- ⁷W. S. Hobson, J. P. van der Ziel, A. F. J. Levi, J. O'Gorman, C. R. Abernathy, M. Geva, L. C. Luther, and V. Swaminathan, *J. Appl. Phys.* **70**, 432 (1991).
- ⁸W. S. Hobson, C. R. Abernathy, S. J. Pearton, and T. D. Harris, *Mater. Res. Soc. Symp. Proc.* **204**, 189 (1991).
- ⁹F. Ren, C. R. Abernathy, S. J. Pearton, T. R. Fullowan, J. Lothian, and A. S. Jordan, *Electron. Lett.* **26**, 724 (1990).
- ¹⁰American Cyanamid Company, Wayne, NJ 07470.
- ¹¹N. G. Paroskevopoulos, S. R. McAfee, and W. S. Hobson (unpublished results).
- ¹²A. G. Mashevskii, M. A. Sinitsyn, D. R. Stroganov, O. M. Fedorova, and B. S. Yavich, *Sov. Tech. Phys. Lett.* **14**, 532 (1988).
- ¹³D. Schmitz, G. Strauch, J. Knauf, H. Jürgensen, M. Heyen, and K. Wolter, *J. Cryst. Growth* **93**, 312 (1988).
- ¹⁴F. Ren, C. W. Tu, R. F. Kopf, C. S. Wu, A. Chandra, and S. J. Pearton, *Electron. Lett.* **25**, 1675 (1989).
- ¹⁵Y. Takanashi and N. Kobayashi, *IEEE Electron Device Lett.* **EDL-6**, 154 (1985).
- ¹⁶M. Abe, T. Mimura, N. Kobayashi, M. Suzuki, M. Kosugi, M. Nakayama, K. Odani, and I. Hanyu, *IEEE Trans. Electron Dev.* **36**, 2021 (1989), and references therein.